Journal of Fluorine Chemistry 131 (2010) 59–65

Contents lists available at ScienceDirect

Journal of Fluorine Chemistry

journal homepage: www.elsevier.com/locate/fluor

Synthesis, structural, spectroscopic and reactivity properties of a new *N*-2,3,4-trifluorophenyl-3,5-di-*tert*-butylsalicylaldimine ligand and its Cu(II) and Pd(II) complexes

Veli T. Kasumov [a,*], Ibrahim Uçar [b], Ahmed Bulut [b]

[a] Department of Chemistry, Harran University, Osmanbey, 63300 Şanlıurfa, Turkey
[b] Department of Physics, Faculty of Arts and Sciences, Ondokuz Mayıs University, 55139 Kurupelit, Samsun, Turkey

ARTICLE INFO

Article history:
Received 17 July 2009
Received in revised form 7 October 2009
Accepted 7 October 2009

Keywords:
Trifluorinated-3,5-di-*tert*-butylsalicylaldimine
Cu(II) and Pd(II) complexes
X-ray structure
Spectroscopy
Chemical oxidation

ABSTRACT

A new *N*-2,3,4-trifluorophenyl-3,5-di-*tert*-butylsalicylaldimine (**1**) complexes with Cu(II) (**2**) and Pd(II) (**3**) have been synthesized and characterized by X-ray crystallography, UV–Vis, IR, ^{1}H NMR and EPR spectroscopic techniques. The X-ray crystal structure of complex **2** reveals tetrahedrally distorted square-planar coordination geometry around Cu(II). The UV/Vis and EPR results indicate that the solid state geometry of **2** remains unchanged in solutions. Chemical oxidation of **3** with Ce(IV) in $CHCl_3$ generates relatively stable Pd(II)–phenoxyl radical complex ($g = 2.0073$). The results related with the chemical oxidation of **2** and **3** as well as the catalytic activity of **3** in the hydrogenation of $PhNO_2$ are presented.

1. Introduction

The design, synthesis and structural characterization of salicylaldimine complexes are a subject of current interest due to their interesting structural, magnetic, spectral, and catalytic and redox properties, use as models for enzymes and various theoretical interests [1–3].

Our interest in these type of complexes was associated with coordination chemistry, electron transfer reactivity and antioxidant effectiveness of *N*-salicylaldimines and other ligands transition metal(II) complexes bearing bulky 2,6-di-*tert*-butylated phenol fragments [4–6]. The unique properties of ligands with these types of bulky phenols are their capability to form stable metal(II)–phenoxyl or semiquinone type radical complexes upon chemical or electrochemical oxidation [3], which are extensively used for elucidating the chemistry and functionality of enzymatic and non-enzymatic processes [7]. In addition, along with unexpected oxidative C–C coupling reactions in the complexation of *N*-1-HO-2,6-di-*tert*-butylphenyl-X-salicylaldimines and other ligands with Cu(II), the reduction of some Cu(II) and Pd(II) complexes in the interaction with tri-arylphosphines [$(XC_6H_5)_3P$] were also observed [4–6].

Our recent studies on coordination chemistry of *N*-X-phenyl(alkyl)-3,5-di-*tert*-butylsalicylaldimines, prepared from 3,5-di-*tert*-salicylaldehyde and mono- (F, Cl, Br, CH_3, OCH_3) and di-substituted (F, Cl, CH_3, OCH_3) aniline derivatives or various n-alkyl(cyclic) amines, demonstrated that they not only easily form bis-ligand chelates only with Cu(II), Co(II) and Pd(II), but they also exhibit less complexing ability with respect to Ni(II), VO(II), Mn(II), Zn(II) and Cd(II) metal ions [8–11]. Our repeated attempts to prepare complexes of these metals with above salicylaldimnes were unsuccessful.

It is interesting to note that in the studies of the catalytic activity of early transition metals complexes (named FI Catalysts) with ligands similar to above, Fujita and co-workers demonstrated that bulky substituents *ortho* to the phenoxy-oxygen in these complexes to play a key role in achieving both living and isospecific polymerization and increase their catalytic activity [12]. Further investigations aimed at developing higher performance FI Catalysts for living ethylene/propylene polymerization led to the discovery of an exceptional fluorinated Ti-FI Catalyst [13]. In order to investigate the mechanism of this unusual polymerization process, complexes which varied in the number and positions of fluorine atoms in imine nitrogen-phenyl group were synthesized [14,15]. The results of the investigations indicate that living

* Corresponding author. Fax: +90 414 3440051.
E-mail address: vkasumov@harran.edu.tr (V.T. Kasumov).

0022-1139/$ – see front matter © 2009 Elsevier B.V. All rights reserved.
doi:10.1016/j.jfluchem.2009.10.005

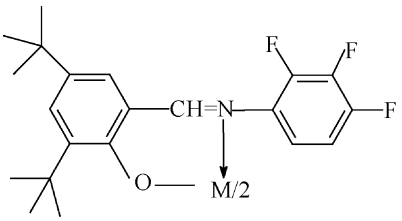

M = Cu(II), Pd(II)

Scheme 1. Structural representations of the $Cu(L)_2$ and $Pd(L)_2$.

polymerizations proceed only when at least one fluorine is located in the 2,6-positions of imine *N*-phenyl group and the activity increases with the number of fluorine atoms in both living and non-living systems. It is reasonable to suggest that electron-withdrawing fluorine enhances the electrophilicity and consequently the living nature stemmed from the stabilization of the Ti center by the *ortho*-F through electronic interaction. However, the calculations indicate that there is no interaction between the Ti center and the *ortho*-F. Instead, the calculations demonstrate that the *ortho*-F interacts electronically with a β-H on a growing polymer chain (*ortho*-F/β-H distance: 2.276 Å) [15,16] indicating that the presence of an attractive interaction between the *ortho*-F and the β-H for all *ortho*-fluorinated Ti-FI independent of the phenoxy-imine ligand structures, confirming the generality of the unusual attractive interaction for *ortho*-F in Ti-FI Catalysts. It should be noted that a similar, but much weaker, interaction has been suggested for the corresponding fluorinated Zr- and Hf-FI Catalysts [12,15].

In continuation, in our studies on the chemistry of sterically hindered phenoxy-imine systems we report the synthesis, crystal structure, spectroscopic characterization, chemical oxidation and catalytic activity of the *N*-2,3,4-trifluorophenyl-3,5-di-*tert*-butyl-salicylaldimine (LH) and its $Cu(L)_2$ and $Pd(L)_2$ complexes (Scheme 1) abbreviated as **1**, **2** and **3**, respectively. It is necessary to note that the chemistry of metal complexes of polyfluorinated Schiff bases is less studied, unlike those of β-diketonate and related ligand chelates [17].

2. Results and discussion

2.1. Structural properties

The molecular structure of **2** including atom-numbering is shown in Fig. 1. Crystal data and additional data collection parameters and refinement details are presented in Table 1. Selected bond distances and angles of **2** as well as the data of hydrogen-bonding interactions are given in Tables 2 and 3, respectively. Complex **2** adopts a tetrahedrally distorted square-planar *trans*-$[CuN_2O_2]$ coordination geometry with O–Cu–O, N–Cu–N and O–Cu–N angles ranges of 92.38(11)–155.73(12)°. The Cu(II) bonds to the two phenolic oxygens and the two imine nitrogens of **1** with a Cu–O distances of 1.894(2), 1.891(2) Å and Cu–N distances of 1.956(3), 1.969(3) Å, respectively. The average Cu–O and Cu–N distances of 1.893(2) and 1.963(3) Å fall within the range reported for other strucurally characterized mononuclear bis-salicylaldimine copper(II) complexes [2,18]. The C7–N1 [1.305(4) Å] and C28–N2 [1.301(4) Å] distances indicate that these correspond to double bonds. The dihedral angle between the two coordination planes defined by Cu1N1O1 and Cu1N2O2 is 36.45(15)° (Fig. 1), as well as the *trans*-O2–Cu1–O1 and *trans*-N2–Cu1–N1 bond angles which are 151.83(12)° and 155.73(12)°, respectively, indicate that the Cu(II) center has a distorted square-planar geometry. The *cis*-O1–Cu1–N1 and O2–Cu1–N1 bond angles are 94.00(11)° and 92.38(11)°, respectively. The dihedral angle between salicylidine ring plane (C8/C9/C10/C11/C12/C13, Ring A) and Cu1/N1/O1 plane is 10.35(15)°, while the same angle between the other salicylidine ring plane (C29/C30/C31/C32/C33/C34, Ring B) and Cu1/N2/O2 plane is 31.39(2)°. The planes of 2-, 3-, 4-F-Ph moieties are approximately perpendicular [81.37(1)°] to each other, whereas the dihedral angle between the salicylidine planes

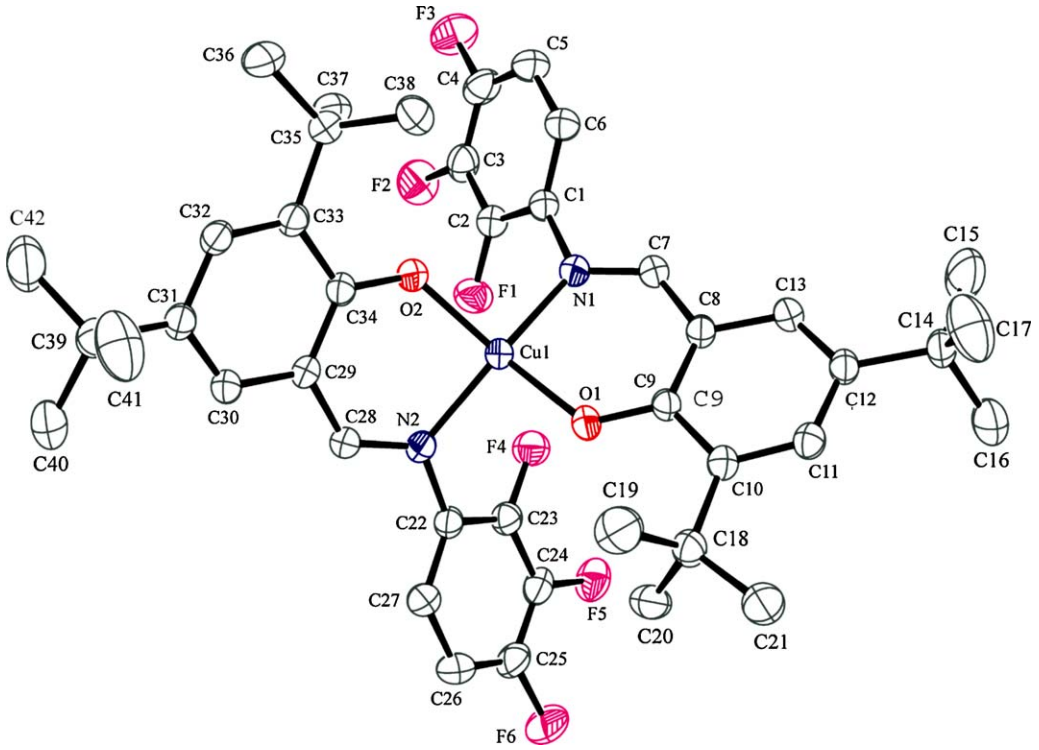

Fig. 1. The molecular structure of **2**, showing the atom-numbering scheme. Displacement ellipsoids are drawn at the 50% probability level and H atom are omitted for clarity.

Table 1
Crystal data and structure refinement for complex **2**.

Formula	$C_{42}H_{46}F_6N_2O_2Cu$
Formula weight	788.36
Temperature (K)	298(2)
Radiation; wavelength	Mo Kα; 0.71073
Crystal system	Monoclinic
Space group	*P* 21/*n*
Unit cell dimensions	
a, *b*, *c* (Å)	9.795(6), 17.635(5), 22.778(11)
α, *β*, *γ* (°)	90.00, 90.144(4), 90.00
Volume (Å^3)	3935(3)
Z	4
Calculated density (g cm^{-3})	1.331
μ (Mo Kα) (mm^{-1})	0.621
F(000), *e*	1644.0
Crystal size (mm)	0.35 × 0.23 × 0.15
θ range (°)	1.46–27.18
h k l ranges	$-12 \le h \le 12$, $-22 \le k \le 22$, $-29 \le l \le 29$
Reflections collected/independent	53644/8710
R_{int}	0.109
Reflections observed [$I > 2\sigma(I)$]	5092
Absorption correction	Integration
Refinement method	Full-matrix least-squares on F^2
Data/restrains/parameters	8710/0/480
Goodness-of-fit on F^2	0.96
*R*1/*wR*2 [$I \ge 2\sigma(I)$]	0.0572/0.1495
*R*1/*wR*2 (all data)	0.1029/0.1685
Final *R* indices [$I > 2\sigma(I)$]	0.057
Largest diff. peak and hole, *e* (Å^{-3})	0.93/−0.65

Table 2
Selected bond lengths (Å) and angles (°) for **2**.

Bond distances (Å)			
N1–Cu1	1.956(3)	C7–N1	1.305(4)
N2–Cu1	1.969(3)	C28–N2	1.301(4)
O1–Cu1	1.894(2)	C28–C29	1.421(5)
O2–Cu1	1.891(2)	C9–O1	1.305(4)
C1–N1	1.426(4)	C34–O2	1.308(4)
Bond angles (°)			
O2–Cu1–O1	151.83(12)	O2–Cu1–N1	92.38(11)
O2–Cu1–N2	92.56(11)	O1–Cu1–N1	94.00(11)
O1–Cu1–N2	94.00(11)	N2–Cu1–N1	155.73(12)

Table 3
Hydrogen-bonding interactions (Å, °).

D–H···A	D–A	H···A	D···A	D–H···A
C6–H6···F6^{ii}	0.93	2.54	3.317(5)	141
C19–H19C···O1	0.96	2.35	2.987(6)	124
C20–H20A···O1	0.96	2.38	3.015(6)	123
C37–H37A···O2	0.96	2.35	3.004(5)	125
C38–H38A···O2	0.96	2.36	2.987(5)	123

Symmetry code (ii): $-1/2+x$, $1/2-y$, $1/2+z$.

is 61.14(12)°. The C9O1Cu1 and C34O2Cu1 angles *α* are 128.5(2)° and 124.1(2)°, respectively, as expected for sp^2-hybridized oxygen atom. Within the layer the shortest non-bridged Cu···Cu distance is 6.94 Å ($-x+1$, $-y$, $-z$).

In extended structure, there are non-classical hydrogen-bonding interactions. The crystal packing of complex **2**, shown in Fig. 2, is formed via intramolecular (C–H···O) and intermolecular (C–H···F) hydrogen bonds (see Table 2 for details), weak π–π and π–ring interactions. π–π stacking is observed between the salicylidine ring B and phenyl (C22/C23/C24/C25/C26/C27; Ring C) moieties of two symmetry related copper(II) complexes. Ring B is oriented in such a way that the perpendicular distance from B to C^i is 3.4529(14) Å, the closest interatomic distance being

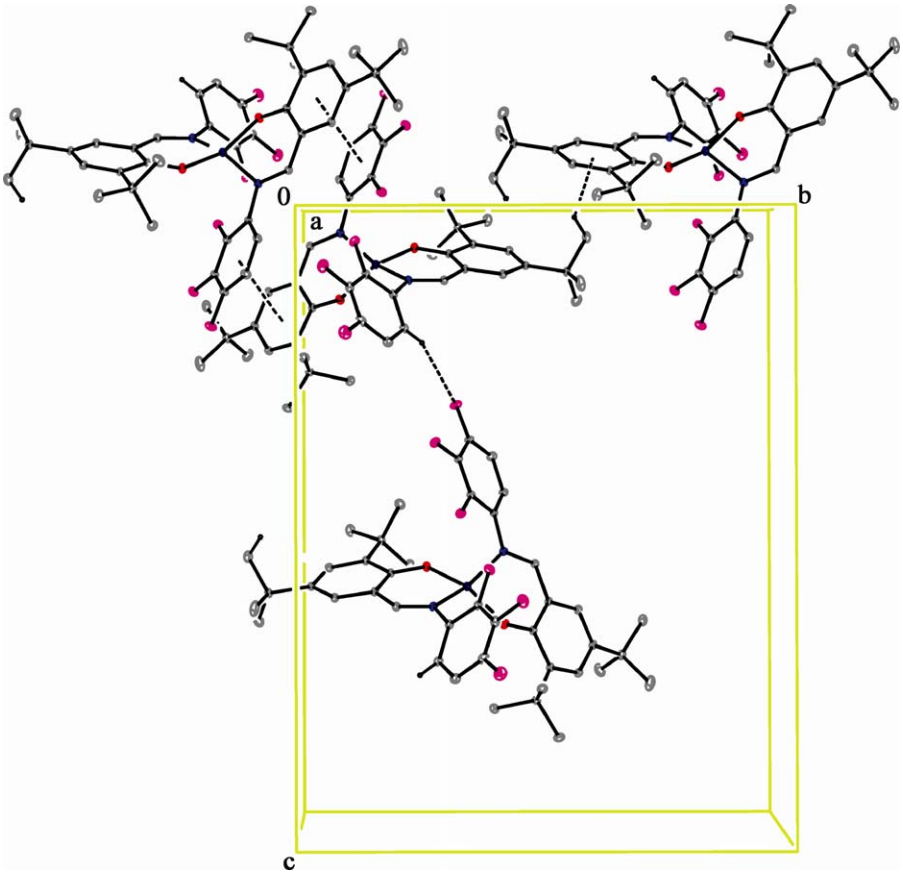

Fig. 2. Packing diagram of complex **2**, showing intermolecular interactions as dashed lines.

C23···C29^{i} [3.466(5) Å; symmetry code (i): $1-x, -y, -z$] are within the range of the sum of the van der Waals radii of two carbon atoms (3.4–3.6 Å) [19], indicating existence π–π stacking interactions between these aromatic rings. The distance between the ring centroids is 3.988(3) Å. In the packing structure of **2** there is also a weak C–H···pi interaction between C16–H16b and a ring A (Fig. 2). The C–H···Cg contact distance between the centroid of a ring A and the H atoms, nearest that ring A, is 2.84 Å. The perpendicular distance between atom H16b and the center of the ring A is 2.74 Å and the C–H···Cg angle is 138°. These intermolecular interactions, namely an extensive network of non-classical hydrogen bonds, π–π stacking and π–ring interactions, are responsible for constructing an infinite three-dimensional lattice in the crystal structure of **2**.

2.2. Spectroscopic properties

Selected IR and UV/Vis data for **1**–**3** compounds are given in Section 4. In the IR spectra of these compounds, there are several sharp bands in the region 2800–3000 cm^{-1} due to the asymmetric and symmetric ν(C–H) stretching frequencies of the $C(CH_3)_3$ groups. The IR spectrum of **1** exhibits a characteristic broad weak band centered in the 2600–2800 cm^{-1} and a sharp strong absorption at 1625 cm^{-1}, attributable to intramolecularly H-bonded phenolic OH and to the ν(CH=N) stretching mode, respectively. In the spectra of complexes, the former band disappears and the latter is shifted to lower frequencies in the spectra of **2** (1612 cm^{-1}) and **3** (1600 cm^{-1}), suggesting the coordination of the imine nitrogen and the deprotonated phenolic oxygen atoms to the metal atom [1].

In the electronic spectrum of **1** in polar hydrogen-bonding solvents such as methanol or ethanol solutions (Section 4), unlike many other substituted similar substituted bidentate arylsalicylaldimines, no absorption was observed around 400 nm, attributable to the ketoamine tautomer structure [20,21]. The higher intense absorption bands observed in the range 210–330 nm and at 362 nm are assigned to intraligand $\pi \rightarrow \pi^*$ and $n \rightarrow \pi^*$, in the aromatic rings and imine groups, respectively. The absence of the visible absorption band around 400 nm, even in concentrated strongly hydrogen-bonding solvents such as EtOH and MeOH, suggests that trifluorinated compound **1** exists only in enol-imine form at room temperature (r.t.). Complex **2** exhibits a phenolate-to-Cu(II) charge-transfer band centered at 415 nm (ε = 19,500 M^{-1} cm^{-1}). A broad band at 665 nm (204 M^{-1} cm^{-1}) is assigned to convolution of three allowed d–d transitions ($d_{x^2-y^2} \rightarrow d_{z^2}$, $d_{x^2-y^2} \rightarrow d_{xz,yz}$ and $d_{x^2-y^2} \rightarrow d_{xy}$), in the tetrahedrally distorted square-planar geometries [22–24]. A strong bands in UV region 250 (sh), 292 (66,000 M^{-1} cm^{-1}) and 337 (sh) are due to of the $\pi \rightarrow \pi^*$ and $n \rightarrow \pi^*$ transitions, respectively.

Complex **3** is diamagnetic, suggesting a square-planar geometry for this complex. Electronic spectra of **3** are also indicative of a square-planar geometry [25]. The electronic spectra of **3** in EtOH and $CHCl_3$ solutions exhibit only two intense bands (*ca.* 300 and 420 nm), which are assigned to metal-to-ligand charge-transfer transitions [22,23]. The DMF solution of **3** also displays very weak shoulder around 500 nm (ε = 275 M^{-1} cm^{-1}) attributable to d–d transition [11].

The ^{1}H NMR spectral characteristics of **1** and **3** are presented in Section 4. The ^{1}H NMR spectrum of **1** in $CDCl_3$ showed strong sharp singlet signals at 1.37 and 1.51 ppm which are assigned to the $C(CH_3)_3$ protons. The trifluorophenyl ring protons signals were observed as two particularly overlapped doublets pattern at 7.04 ppm. Two doublets, observed at 7.26 and 7.54 ppm, are assigned to *meta*-coupled salicylidine ring C_4–H and C_6–H hydrogen atoms resonances. The CH=N and OH groups protons resonances appeared as singlet peaks at 8.88 and 13.18 ppm, respectively. The ^{1}H NMR spectrum of **3** showed single resonances at δ = 0.96, 1.24, and 7.08 ppm, which are assigned to the $C(CH_3)_3$ and CH=N protons. The multiplet pattern at 6.94–7.07 ppm is assigned to resonances of trifluorophenyl non-equivalent protons. Two doublet signals centered at 7.26 and 7.54 ppm are assigned to *meta*-coupled salicylidine ring protons. The comparison of the ^{1}H NMR spectrum of **1** with that for **3** indicates that the complexation of **1** by Pd(II) is accompanied by the high field shifts of the resonances of protons in the imine ($\Delta\delta \sim 0.9$ ppm), trifluorophenyl ($\Delta\delta \sim 0.5$ ppm) and *tert*-butyl ($\Delta\delta \sim 0.27$ ppm) groups. On the other hand, the ring C_4H and C_6H protons resonances at lower fields comparing to free ligand protons.

The observed r.t. magnetic moment of **2** (1.83 B.M.) per Cu(II) ion is consistent with the magnetic moment data reported for tetrahedrally distorted square-planar Cu(II) complexes [22,23]. The room temperature ESR spectrum of powder samples of **2**, is characterized by an axial g tensors with $g_{||}$ (2.223) > $g_{\perp}$ (2.072) > g_e. The solution ERP spectrum of this complex in $CHCl_3$ displays isotropic (298 K) (g_{iso} = 2.116, A_{iso} = 73.3G) and anisotropic (173 K) ($g_{||}$ = 2.232, $g_{\perp}$ = 2.058, $A_{||}$ = 168G and $A_{\perp}$ = 26G) signals, which are typical for monomer copper(II) complexes. The observed trend, $g_{||} > g_{\perp} > g_e$, suggests a $d_{x^2-y^2}$ or d_{xy} ground state in a distorted copper centers for **2** [22]. The obtained ratio $g_{||}/A_{||}$ (142 cm) for **2**, lying between 140 and 250 cm, again indicates tetrahedral distorted square-planar environment for Cu(II) centers in frozen CHCl3 solution [26]. The exchange-coupling parameter, $G = (g_{||} - g_e)/(g_{\perp} - g_e)$, reflects the exchange interaction between the copper(II) centers in polycrystalline solids [22]. According to Hathaway and Billing [22], if $G > 4$ the exchange interaction is negligible. A value of $G < 4$ indicates considerable exchange interaction in the solid complex. The obtained value G = 3.17 for powder samples of **2**, unlike its frozen glass $CHCl_3$ solution samples which has a G value of 4.12, suggests the presence of an exchange coupling interaction between Cu(II) centers in the solid state [22].

2.3. Chemical oxidation of 2 and 3

Our recent studies demonstrated that in the chemical oxidation of some bis(*N*-X-aryl-(alkyl)-3,5-di-*tert*-butylsalicylaldiminato)Cu(II) complexes by $(NH_4)_2Ce(NO_3)_6$ [Ce(IV)] in $CHCl_3$ along with a decrease of the intensity of their EPR spectra, the appearance of radical signals takes place [8–11]. A similar EPR and UV/Vis investigation of the oxidative behavior of **1**–**3** compounds was performed in the present work. The spectral changes followed by the chemical oxidation of **2** with Ce(IV) in CH_3CN and $CHCl_3$ solutions at r.t. and under aerobic conditions, were monitored by UV/Vis spectroscopy in the range 200–1100 nm. One-electron oxidation of **2** (5.5×10^{-3} M) in MeCN with one equiv Ce(IV), along with color change from dark brown to yellowish brown, is accompanied by the simultaneous disappearance of the d–d absorption band of the parent complex **2** at 660 nm and the growth of a new broad band of lower intensity maxima at 708 nm was observed (Fig. 3a). Upon successive recording of this band with time interval of 1 min, the shifts of this band to a lower wavelength with decreased absorbance, λ_{max}(A), from 708 (0.61) to 695 (0.51) nm within a period 5 min were detected. In the following repeated scanning, slowly decreases in the intensity and blue shifts were detected. It is interesting that in the oxidation of concentrated **2** (1.2×10^{-2} M) by one or two equiv Ce(IV), scanning after 30 s, the appearance of additional band at $\lambda > 1100$ nm was observed (Fig. 3b). After the second scan this band was disappeared. This observation suggests that the generated $[\mathbf{2}^{\bullet}]^{+}$ or $[\mathbf{2}^{\bullet\bullet}]^{++}$ primer radical cation complexes are unstable and rapidly decompose under experimental conditions, at 290 K.

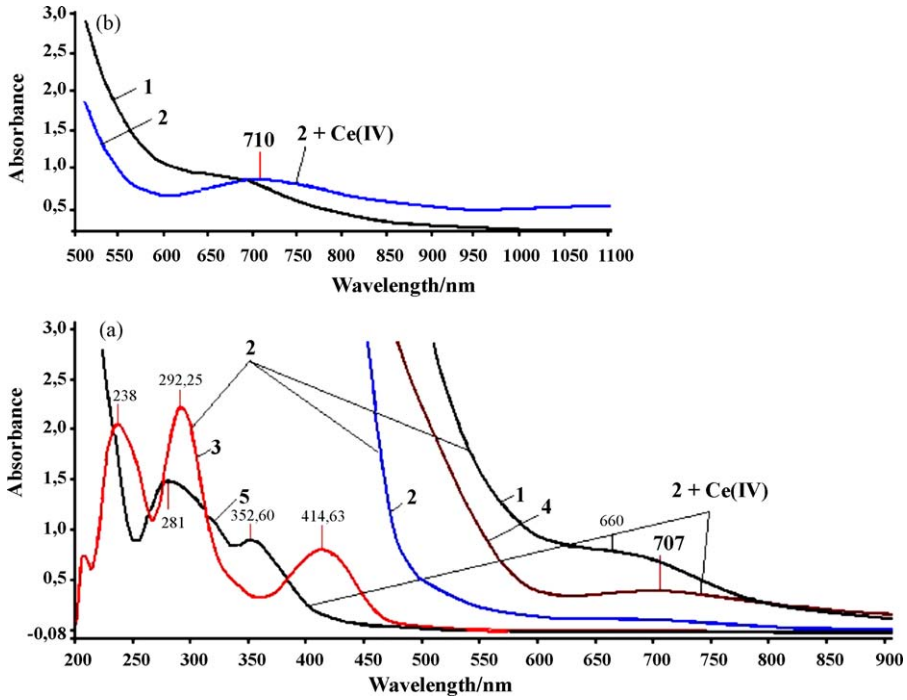

Fig. 3. UV/Vis spectra of **2**: (a) absorption bands of initial complex **2** (1, 2 and 3) in CH_3CN; absorption spectral change of **2** (3.8×10^{-3} M) after one-electron oxidation by 2 equiv of Ce(IV) at 290 K in CH_3CN (4 and 5); (b) Initial spectrum of relatively concentrated **2** (1.12×10^{-2} M) (1) in CH_3CN; spectrum of **2** + 2 equiv Ce(IV) system (2) scanned after 30 s at 290 K in CH_3CN.

Upon addition of two equiv molar Ce(IV) into CH_3CN solution of **3**, without appearance of any new bands in the visible region, the color change from orange to red was observed. At the same time, in the similar treatment of **3** in $CHCl_3$ solution at r.t., even in the presence of atmospheric oxygen, the appearance of singlet signal with $g = 2.0073$ ($\Delta H = 28G$) was detected. The relatively stable behaviors and the increased g-factors of these radicals compared to that for free 2,4-di-*tert*-butylphenoxyl radical ($g = 2.0045$) [27], suggest significant metal-orbital contribution to the SOMO of phenoxyl radical and also that the generated radical species can be assigned to Pd(II)–phenoxyl radical complexes.

2.4. Catalytic reduction of nitrobenzene by 3 complex

The hydrogenation reaction of nitrobenzene with catalyst **3** was carried out at atmospheric pressure in a magnetically stirred glass reactor using DMF as solvent. The progress of the reduction of nitrobenzene was followed by measuring the uptake of hydrogen gas as a function of the reaction time, at constant pressure, using a glass manometer. The catalytic studies showed that complex **3** exhibits a catalytic activity towards the hydrogenation of nitrobenzene in DMF solution at 20 and 30 °C, under normal pressure of H_2 gas (760 Torr), without any preliminary activation. The concentration of nitrobenzene was varied from 0.147 to 1.224 mol/l at 30 °C and 1 atm H_2 pressure using a fixed amount of the catalyst (3.15×10^{-4} mol/l) Pd(II) content. In order to check whether the catalyst lost its activity or not, the recycling efficiency of the catalysts was carried out by conducting some experiments over a period of 24 h. It was observed that the initial rate of hydrogenation reaction remains almost unchanged even after 36 h (Fig. 4). The recycling experiments showed that the catalytic activity of **3** remains unchanged and can be reused without appearance any sign of decomposition of complex. Unlike mono-fluoro-substituted Pd(*N*-X-arylsalicylaldimiato)$_2$ type complexes [10], no evidence of the palladium metal precipitation was observed in the course of the hydrogenation of nitrobenzene for a period of 36 h. The average rate of H_2 absorption and the specific catalytic activity of **3** were obtained as 0.8 ml/min and 6.58 H_2 consumed/mol-cat(min), respectively.

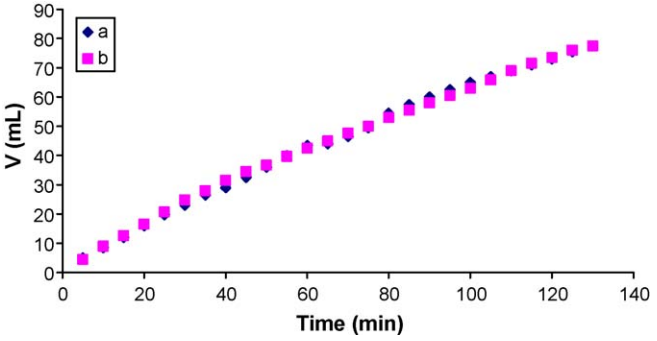

Fig. 4. Hydrogenation of $PhNO_2$ with catalyst **3** (3.1×10^{-4} M, 6.2×10^{-6} mol) in 20 ml DMF at 303 K: (a) $C_{PhNO_2} = 0.147$ M; (b) $C_{PhNO_2} = 1.205$ M.

3. Conclusions

New copper(II) and palladium(II) complexes of *N*-2,3,4-trifluorophenyl-3,5-di-*tert*-butylsalicylaldimine ligand were synthesized and characterized by spectroscopic and X-ray crystallography. The presented ligand possesses lower complexation ability towards Co(II), Ni(II), Mn(II), VO(II) and Zn(II). The X-ray study shows that the geometry around copper(II) atoms is tetrahedrally distorted square-planar. As supported by EPR and UV/Vis studies, their chemical oxidation with Ce(IV) leads to the formation of the relatively stable metal(II)–phenoxyl radical complexes. It has been demonstrated that trifluorinated sterically hindered Pd(II) complex exhibits catalytic activity in the hydrogenation of nitrobenzene without losing activity at least for 3 months.

4. Experimental

4.1. Materials

All solvents, sulfuric acid, acetic acid, hexamethylenetetramine, nitrobenzene, 2,4-di-*tert*-butylphenol, $(NH_4)_2Ce(NO_3)_6$, 2,3,4-trifluoroaniline and acetates of Cu(II) and Pd(II) were purchased from Sigma–Aldrich and used without further purification. The reagent 3,5-di-*tert*-butylsalicylaldehyde was prepared according to the literature procedure [28].

4.2. Instrumentation

The C, H, N elemental analyses were performed on a LECO CHNS-932 model analyzer. Electronic spectra were recorded by using a PerkinElmer Lambda 25 spectrometer, IR spectra obtained on a PerkinElmer FT-IR spectrometer using KBr pellet. ^{1}H NMR spectra were recorded on a Bruker Spectro spin Avance DPX-400 Ultra Shield Model NMR with Me_4Si as an internal standard in $CDCl_3$. The room temperature magnetic susceptibility was measured by using a Sherwood Scientific magnetic balance and the diamagnetic corrections were evaluated using Pascal's constant. ESR spectra were taken on a Varian E109C X-band spectrometer. The field and frequency calibration were made using DPPH (g = 2.0037).

4.3. Synthesis

4.3.1. N-2,3,4-trifluorophenyl-3,5-di-tert-butylsalicylaldimine (1)

Ligand **1** was prepared using standard procedures involving the condensation of 3,5-di-*tert*-butyl-2-hydroxybenzaldehyde (0.936 g, 4 mmol) with 2,3,4-fluoroaniline (0.588 g, 4 mmol) in absolute ethanol (100 ml) in the presence of a few drops of formic acid. The mixture was stirred at reflux for 36 h and then concentrated to ~40 ml. By slow cooling of the reaction mixture to room temperature, a light yellow crystal of **1** was obtained. Yield 1.277 g, 88%. mp = 102 °C. IR (KBr, cm^{-1}): 1625 (CH=N), 2866–2957 [C(CH$_3$)$_3$]; UV/Visible [EtOH, λ_{max}/nm (log ε)]: 225(4.47), 234(sh), 282(4.5), 322(sh), 360(4.1). ^{1}H NMR (300 MHz, $CDCl_3$), δ: 13.18 (s, 1H, OH), 8.88 (s, 1H, CH=N), 7.537 (d, J = 2.1 Hz, 1H, *meta*-coupled 4-Ar*H*), 7.255 (d, J = 2.4 Hz, 1H, *meta*-coupled 6-Ar*H*), 7.018 (d, J = 5.7 Hz, 1H, 2,3,4-F-Ph C6-*H*), 7.049 (d, J = 5.4 Hz, 1H, 2,3,4-FPh C5-*H*), 1.51 (s, 9H), 1.367 (s, 9H). Anal. calcd. for $C_{21}H_{24}NOF_3$: C, 73.02; H, 7.29; N, 4.05. Found: C, 72.74; H, 7.29; N, 4.18.

4.3.2. Copper bis{2-[(2,3,4-Trifluorophenylimino)methyl-3,5-di-tert-butylphenolato]} (2)

Complex **2** was prepared by addition of 5 ml methanol solution of $Cu(OAc)_2xH_2O$ (0.1 g, 0.5 mmol) to a hot solution of MeOH (60 ml) containing **1** (0.364 g, 1.0 mmol). The reaction mixture was refluxed with stirring for *ca.* 60 min. Then the volume of solution was reduced to ~30 ml and kept in air at r.t. After one day the dark green crystals were obtained.

Crystals of **2** suitable for an X-ray crystal structure determination were grown from a saturated solution of methanol at r.t. Yield 0.295 g, 74.7%. mp > 270 °C. FT-IR (KBr, cm^{-1}): 2868–2952 [C(CH$_3$)], 1612 (CH=N), 3429 (OH, lattice H_2O)]. UV–Vis ($CHCl_3$, λ_{max}/nm (log ε): 250(sh), 292(4.82), 337(sh), 415(4.29), 665(2.31), μ_{eff} = 1.83μ_B. Anal. calcd. for $C_{42}H_{46}N_2O_2F_6Cu$: C, 67.08; H, 6.43; N, 3.72; Found: C, 66.81; H, 6.73; N, 3.08.

4.3.3. Palladium bis{2-[(2,3,4-Trifluorophenylimino)methyl-3,5-di-tert-butylphenolato]} (3)

Complex **3** was prepared by direct addition of $Pd(OAc)_2$ (0.112 g, 0.5 mmol) to 30 ml hot CH_3CN solution of **1** (0.363 g, 1 mmol) and stirred at ~40 °C for *ca.* 45 min. Yield 0.284 g, 68%. mp > 310 °C. Anal. calcd. for $C_{42}H_{46}N_2O_2F_6Pd$: C, 60.68; H, 5.57; N, 3.37. Found: C, 60.07; H, 5.48; N, 3.19. FT-IR (KBr, cm^{-1}): 2868–2958 [C(CH$_3$)$_3$], 1600 (CH=N); UV–Vis [EtOH, λ_{max}/nm (log ε)]: 231(4.66), 261(3.74), 304(3.52), 414(3.17). ^{1}H NMR (300 MHz, $CDCl_3$): δ 7.08 (s, 2H, CH=N), 7.555 (d, J = 1.5 Hz, 2H, *meta*-coupled 4-Ar*H*), 7.315 (d, J = 2.4 Hz, 2H, *meta*-coupled 6-Ar*H*), 7.11–6.94 (m, 4H, 2,3,4-FPh*H*), 1.24 [s, 18H, C(C*H*$_3$)$_3$), 0.9 (s, 18H, C(C*H*$_3$)$_3$].

4.4. X-ray structural determination of 2

A suitable single crystal of complex **2** was mounted on a glass fiber and data collection were performed on a STOE IPDS(II) image plate detector using Mo Kα radiation (λ = 0.71019 Å) at 298 K. Data collection: Stoe X-AREA [29]. Cell refinement: Stoe X-AREA [29]. Data reduction: Stoe X-RED [29]. The structure was solved by direct methods using SHELXS-97 [30] and anisotropic displacement parameters were applied to non-hydrogen atoms in a full-matrix least-squares refinement based on F^2 using SHELXL-97 [30]. All hydrogen atoms except H7 and H28 were positioned geometrically and refined by a riding model with U_{iso} 1.2 times that of attached atoms and remaining hydrogen atoms were found by Fourier difference. Molecular drawings were obtained using ORTEP-III [31].

Acknowledgment

We are grateful to the Harran University Research Council for Grant under HÜBAK-712.

Appendix A. Supplementary data

Crystallographic data (excluding structure factors) for the structure in this paper have been deposited with the Cambridge Crystallographic Data Centre as the supplementary publication no. CCDC 718000 for 2. These data can be obtained free of charge on application to CCDC, 12 Union Road, Cambridge, CB12 1EZ, UK, fax: +44 1223 366 033, e mail: deposit@ccdc.cam.ac.uk or on the web www: http://www.ccdc.cam.ac.uk.

References

[1] R.H. Holm, M.J. O'Connor, Prog. Inorg. Chem. 14 (1971) 241–401.
[2] A.D. Garnovski, A.P. Sadimenko, M.C. Sadimenko, D.A. Garnovski, Coord. Chem. Rev. 173 (1998) 31–77.
[3] P. Chaudhuri, K. Wieghardt, Prog. Inorg. Chem. 50 (2001) 151–216.
[4] A.A. Medjidov, V.T. Kasumov, H.S. Mamedov, Koord. Khim. 7 (1981) 66–71.
[5] A.A. Medjidov, V.T. Kasumov, M.K. Guseyinova, H.S. Mamedov, V.S. Aliev, Dokl. AN USSR 259 (1981) 866–869.
[6] V.T. Kasumov, A.A. Medjidov, Koord. Khim. 15 (1989) 1404–1407.
[7] I.J. Rehle, T.F. Markle, H. Nagao, A.G. DiPasquale, O.P. Lam, M.A. Lockwood, K. Rotter, J.M. Mayer, J. Am. Chem. Soc. 128 (2006) 6075–6088, and references therein.
[8] V.T. Kasumov, F. Köksal, R. Köseoglu, J. Coord. Chem. 57 (2004) 591–603.
[9] V.T. Kasumov, F. Köksal, Y. Zeren, Spectrochim. Acta Part A 63 (2006) 330–336.
[10] V.T. Kasumov, F. Köksal, A. Sezer, Polyhedron 24 (2005) 1203–1211.
[11] V.T. Kasumov, E. Taş, F. Köksal, Ş Özalp-Yaman, Polyhedron 24 (2005) 319–325.
[12] H. Makio, N. Kashiwa, F. Fujita, Adv. Synth. Catal. 344 (2002) 477–493.
[13] A.F. Mason, J. Tian, P.D. Hustad, E.B. Lobkovsky, G.W. Coates, Isr. J. Chem. 42 (2002) 301–306.
[14] R. Furuyama, J. Saito, S. Ishii, H. Makio, M. Mitani, H. Tanaka, T. Fujita, J. Organomet. Chem. 690 (2005) 4398–4413.
[15] T. Matsugi, T. Fujita, Chem. Soc. Rev. 37 (2008) 1264–1277.
[16] K. Kawai, T. Fujita, Top. Organomet. Chem. 26 (2009) 3–46.
[17] D.L. Chizhov, D.V. Sevenard, E. Lork, K.I. Pashkevich, G.V. Röschenthaler, J. Fluorine Chem. 123 (2004) 1137–1141.
[18] S. Yamada, Coord. Chem. Rev. 190–192 (1999) 537–555.
[19] A. Bondi, J. Phys. Chem. 68 (1964) 441–451.
[20] M.D. Cohen, G.M.J. Schmidt, J. Phys. Chem. 66 (1962) 2442–2446.
[21] Y.I. Koslov, D.N. Shigorin, R.N. Nurmukametov, V.A. Puchkov, Russ. J. Phys. Chem. 37 (1963) 1315–1319.

[22] B.J. Hathaway, D.E. Billing, Coord. Chem. Rev. 6 (1970) 143–207.
[23] L. Sacconi, M. Ciampolini, J. Chem. Soc. (1964) 276–281.
[24] B. Bosnich, J. Am. Chem. Soc. 90 (1968) 627–632.
[25] P.L. Googgin, R.J. Goodfellow, F.J.S. Reed, J. Chem. Soc., Dalton Trans. (1972) 1298–1303.
[26] U. Sakaguchi, A.W. Addison, J. Chem. Soc., Dalton Trans. (1979) 600–608.
[27] B.A. Jazdzewski, W.B. Tolman, Coord. Chem. Rev. 200–202 (2000) 633–685.
[28] J.F. Larrow, E.N. Jacobsen, Y. Gao, Y. Hong, X. Nie, C.M. Zeppe, J. Org. Chem. 50 (1994) 50–56.
[29] Stoe & Cie X-AREA (Version 118) and X-RED (Version 104), Stoe & Cie, Darmstadt (Germany) 2002.
[30] G.M. Sheldrick, SHELXL-97, Program for the Refainment of Crystal Structures, University of Gottingen, Germany, 1997.
[31] M.N. Burnett, C.K. Johnson, ORTEP III, Report ORNL-6895, Oak Ridge National Laboratory, TN, USA, 1996.